Modelling of Swimming Posture Dynamics for a Beaver-like Robot

Modelling of Swimming Posture Dynamics for a Beaver-like Robot

Gang Chen [a, b *], Zhenyu Wang [a], Jiajun Tu [c], Huosheng Hu [b], Donghai Wang [a *]

[a] Faculty of Mechanical Engineering and Automation, Zhejiang Sci-Tech University, Hangzhou 310018, China

[b] School of Computer Science and Electronic Engineering, University of Essex, Colchester CO4 3SQ, U.K.

[c] Faculty of Intelligent Manufacturing, Jiaxing Vocational & Technical College, Jiaxing 314000, China

*Corresponding author, Email: gchen@zstu.edu.cn

Abstract:

Bionic underwater robot swims to generate its propulsion in water which in turn directly determines its moving stability. It is important to explore the relationship between the swimming force and the posture. This paper aims to analyse and model the swimming posture dynamics of a beaver-like robot. The posture dynamics is decomposed into three parts: leg dynamics, body hydrodynamics and body posture dynamics. First, the leg dynamics model of beaver-like robot is established by rigid-fluid integration method. Then, the body hydrodynamics is modelled by numerical calculation method to obtain the water force on the body during swimming. Finally, the swimming posture dynamics model of the robot is constructed to describe the relationship between the leg movement and body posture. The swimming process of beaver-like robot with bionic alternating and synchronous trajectory is simulated with ADAMS. The proposed modelling method and the swimming posture dynamics model are verified by comparing the simulation and theoretical calculation results of robot posture, which could be used for the swimming posture control of a bionic underwater robot.

Keywords: Swimming posture dynamics, Rigid-fluid integration dynamics, Hydrodynamics, Bionic robot, Beavers

1. Introduction

Aquatic and terrestrial animals have different body shapes and motion modes, resulting in different swimming forms. For instance, birds swim by paddling fins [1], fishes move by swinging their bodies and caudal fins[2, 3], turtles and crabs go forward by flapping[4], squid

and jellyfish move by changing their cavities with water jets[5], and frogs swim with flippers[6, 7]. Amphibians mostly move forward with their legs[8, 9]. Legs have multiple joints and webbed feet, which maintain high flexibility and propulsion efficiency. Up to now, different forms of amphibian-like robots have been developed. Zou et al. designed walking and swimming feet and skeleton of the bionic amphibian crab robot. Chen et al. studied the movement mechanism and bionic mechanism synthesis of amphibian-like turtle robot to implement motion mode switching in different environments. Gul et al. used multi-layer 3D printing to build a soft frog robot with embedded shape-memory alloy and flex sensors.

Underwater robot with webbed feet swims by paddling its legs and to generate propulsion force. The stability of underwater robot's swimming posture directly affects the accuracy of underwater swimming trajectory. Its body flexibility is important to the underwater detection and operation of the robot. Li et al. proposed a general multi-body dynamics algorithm to solve various fish swimming problems, including sub-propulsion multi-DOF and rigid undulating body, and undulating body with multiple deformable fins. Yu et al. analysed the flow force of robotic fish with Morrison equation and bar method. Christopher et al. proposed a dynamic model of webbed paddling of a frog-like robot, which was suitable for various sizes and complex hydrodynamic problems such as aquatic insects or fish fins. It should be noticed that the research on swimming dynamics of underwater bionic robot was focused on the force analysis of one leg or part of the body instead of the overall study on the swimming posture dynamics of underwater bionic robot.

In this paper, the swimming posture dynamics of a beaver-like underwater robot is studied to explore the influence of the swimming force on the robot posture. The rest content of this paper is organized as follows. In Section 2, the leg kinematics model of a beaver-like underwater robot is established. Section 3 analyses the swimming posture dynamics of beaver-like underwater robot. Simulations of swimming posture dynamics of the robot are conducted to verify the dynamics model method in Section 4. Swimming experiments are presented in Section 5. Finally, a brief conclusion and future work are given in Section 6.

2. Beaver-like underwater robot and kinematics model

2.1 Beaver-like underwater robot platform

Beavers are amphibians, mainly inhabiting in Europe, as well as living in Qinghe river, Buergen River and Wulungu River in northeast Xinjiang of China. As shown in Fig. 1, it has large body, short neck, short forelimbs with small feet and strong claws. Its hind limbs are strong with webbed feet and its tail is big and flat. It can swim flexibly under water and walk on land.

Fig.1 Beaver[10]

Fig. 2 shows a beaver-like robot developed by our research team, which has three parts: forelimbs, body and hind limbs. The forelimbs include the thigh, calf, hip and knee joint. The streamlined body connects the limbs and is equipped with an Arduino-based robot controller. The hind limbs consist of thigh, calf, webbed feet, and hip, knee and ankle joints. The three joints have a rotational degree of freedom respectively. The webbed foot extends and contracts with a rope actuated mechanism. Its body is 280 mm long, 258 mm wide and 360 mm high. The thigh and calf of the forelimb are 100 mm and 125 mm long respectively. The thigh and calf of the hind limb are 132 mm and 138 mm long. The total mass of the robot is 4.2 kg in air.

(a) (b)

Fig. 2 Beaver-like robot platform being developed

2.2 Kinematics model of beaver-like robot

2.2.1 Kinematic coordinate system

Fig. 3 shows the kinematic coordinate system of our beaver-like robot, which describes

the motion (displacement and posture) of the robot in six degrees of freedom in swimming. The displacement includes x, y, and z, which represent the forward, swing and diving motion, and the posture includes θ, φ, ϕ which represent the pitch, heading and roll motion respectively.

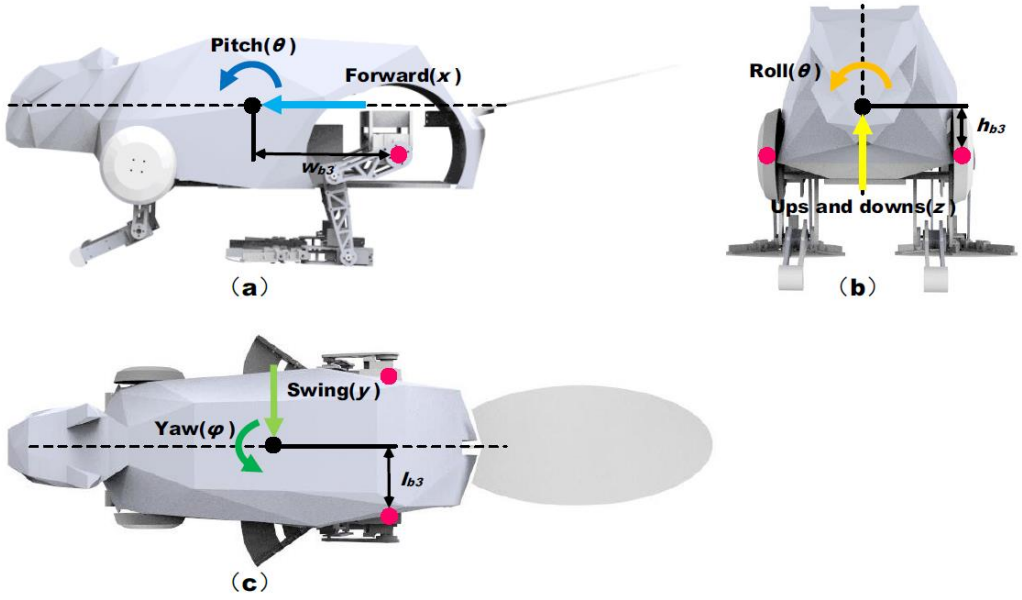

Fig. 3 Coordinate diagram of our beavers like robot

Table 1 Parameter definition of our beaver-like robot

	Position and attitude	Linear velocity and angular velocity	Force and moment
Translation in X direction (forward)	x	u	X
Translation in the Y direction(swing)	y	v	Y
Translation in the Z direction (up-down)	z	w	Z
Rotation about X axis (roll)	ϕ	p	K
Rotation about the Y-axis (pitch)	θ	q	M
Rotation about the Z-axis (yaw)	φ	r	N

Table 1 defines the relative symbolic variables of the pose, linear and angular velocity, force and moment of the beaver-like robot in the corresponding coordinate system. These variables are used to describe the changes of position and posture, linear velocity and angular velocity, force and torque during robot movement. η, v, τ represent the posture, velocity/angular

velocity and force/torque of the robot under 6 DOFs respectively, which are shown below.

$$\eta = [x, y, z, \phi, \theta, \psi]^T$$
$$v = [u, v, w, p, q, r]^T$$
$$\tau = [X, Y, Z, K, M, N]^T$$

2.2.2 Leg Kinematics modelling

Fig. 4 shows the leg kinematics model of the beaver-like robot, which has a total of three degrees of freedom. This model transfers the velocity of body and leg movement to the end webbed foot, which are used to calculate the dynamic force generated in swimming. The leg linkage rotates around the Z axis. D-H parameters of the robot leg are shown in Table 2.

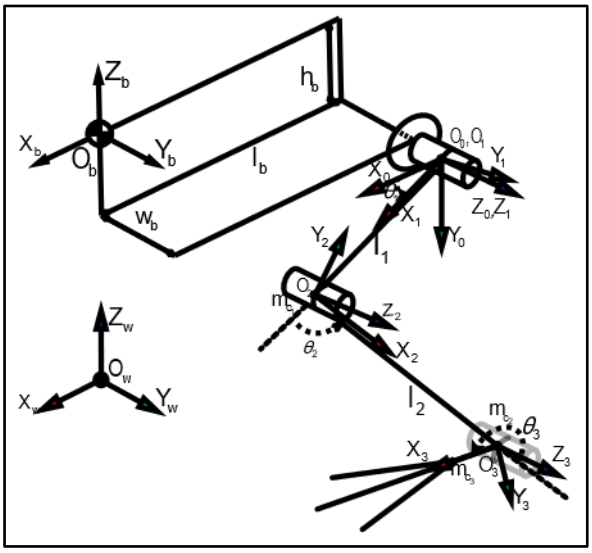

Fig. 4 Kinematics model of leg of beaver-like underwater robot

Table 2 D-H parameters of legs of beaver-like underwater robot

Joints *i*	α_{i-1}	a_{i-1}	d_i	θ_i
0	0	0	0	0
1	0	l_1	0	θ_1
2	0	l_2	0	θ_2
3	0	l_3	0	θ_3

The position vector of the centre of mass for each linkage rod is defined as follows:

$$ {}^{1}p_{c1} = l_1 \hat{X}_1 \tag{2-1} $$

$$ {}^{2}p_{c_2} = l_2 \hat{X}_2 \tag{2-2} $$

$$ {}^{3}p_{c_3} = l_3 \hat{X}_3 \tag{2-3} $$

The material density of linkage is very low, and the relatively heavy motor is located at the joint so that the mass of linkage is concentrated at the joint. The inertia tensor of the centre of mass of each linkage is 0 matrix, and the rotation matrix between adjacent coordinate systems is as follows.

$$ {}^{1}_{0}R = \begin{bmatrix} c_1 & s_1 & 0 \\ -s_1 & c_1 & 0 \\ 0 & 0 & 1 \end{bmatrix} \tag{2-4} $$

$$ {}^{2}_{1}R = \begin{bmatrix} c_2 & s_2 & 0 \\ -s_2 & c_2 & 0 \\ 0 & 0 & 1 \end{bmatrix} \tag{2-5} $$

$$ {}^{3}_{2}R = \begin{bmatrix} c_3 & s_3 & 0 \\ -s_3 & c_3 & 0 \\ 0 & 0 & 1 \end{bmatrix} \tag{2-6} $$

3. Swimming posture dynamics of beaver-like robot

3.1 Dynamic modelling of legs

When a beaver-like robot swims in water, its leg joints rotate and actuate the webbed foot paddling, thus generating the forward propulsion. The length of the thigh and calf l_1, l_2, and the mass is m_1, m_2 respectively. The mass of the webbed foot is m_{c_1}, m_{c_2}, m_{c_3}. linkage is We define the body as joint 0 and its velocity and acceleration parameters are calculated by

$$ \omega_0 = 0 \tag{3-1} $$

$$ \dot{\omega}_0 = 0 \tag{3-2} $$

$$ {}^{0}v_0 = \begin{bmatrix} v_{c_0} \\ 0 \\ 0 \end{bmatrix} \tag{3-3} $$

where v_{c_0} is the velocity at the centre of mass.

$$ {}^{0}\dot{v}_0 = \begin{bmatrix} 0 \\ g \\ 0 \end{bmatrix} \tag{3-4} $$

Hip joint is defined as joint 1. Its velocity and acceleration models are established by

$$ \omega_1 = {}^{1}_{0}R\omega_0 + \dot{\theta}_1\hat{Z}_1 = \begin{bmatrix} 0 \\ 0 \\ \dot{\theta}_1 \end{bmatrix} \tag{3-5} $$

$$ \dot{\omega}_1 = {}^{1}_{0}R\dot{\omega}_0 + {}^{1}_{0}R\omega_0 \times \dot{\theta}_1\hat{Z}_1 + \ddot{\theta}_1\hat{Z}_1 = \begin{bmatrix} 0 \\ 0 \\ \ddot{\theta}_1 \end{bmatrix} \tag{3-6} $$

$$ {}^{1}v_1 = {}^{1}_{0}R\left(\omega_0 \times P_1 + {}^{0}v_0\right) = \begin{bmatrix} v_{c_0}c_1 \\ -v_{c_0}s_1 \\ 0 \end{bmatrix} \tag{3-7} $$

$$ {}^{1}\dot{v}_1 = {}^{1}_{0}R\left(\dot{\omega}_0 \times {}^{0}p_1 + \omega_0 \times \left(\omega_0 \times {}^{0}p_1\right) + {}^{0}\dot{v}_0\right) = \begin{bmatrix} gs_1 \\ gc_1 \\ 0 \end{bmatrix} \tag{3-8} $$

$$ v_{c_1} = \dot{\omega}_1 \times {}^{1}P_{c_1} + \omega_1 \times \left(\omega_1 \times {}^{1}P_{c_1}\right) + {}^{1}\dot{v}_1 = \begin{bmatrix} -l_1\dot{\theta}_1^{\,2} + gs_1 \\ l_1\ddot{\theta}_1 + gc_1 \\ \ddot{\theta}_1 \end{bmatrix} \tag{3-9} $$

The knee joint is defined as joint 2. Its velocity and acceleration models are established by

$$ \omega_2 = {}^{2}_{1}R\omega_1 + \dot{\theta}_2\hat{Z}_2 = \begin{bmatrix} c_2 & s_2 & 0 \\ -s_2 & c_2 & 0 \\ 0 & 0 & 1 \end{bmatrix}\begin{bmatrix} 0 \\ 0 \\ \dot{\theta}_1 \end{bmatrix} + \begin{bmatrix} 0 \\ 0 \\ \dot{\theta}_2 \end{bmatrix} = \begin{bmatrix} 0 \\ 0 \\ \dot{\theta}_1 + \dot{\theta}_2 \end{bmatrix} \tag{3-10} $$

$$ \dot{\omega}_2 = {}^{2}_{1}R\dot{\omega}_1 + {}^{2}_{1}R\omega_1 \times \dot{\theta}_2\hat{Z}_2 + \ddot{\theta}_2\hat{Z}_2 = \begin{bmatrix} c_2 & s_2 & 0 \\ -s_2 & c_2 & 0 \\ 0 & 0 & 1 \end{bmatrix}\begin{bmatrix} 0 \\ 0 \\ \ddot{\theta}_1 \end{bmatrix} + \begin{bmatrix} 0 \\ 0 \\ \ddot{\theta}_2 \end{bmatrix} = \begin{bmatrix} 0 \\ 0 \\ \ddot{\theta}_1 + \ddot{\theta}_2 \end{bmatrix} \tag{3-11} $$

$$ {}^{2}v_2 = {}^{2}_{1}R\left(\omega_1 \times {}^{1}P_2 + {}^{1}v_1\right) = \begin{bmatrix} c_2 & s_2 & 0 \\ -s_2 & c_2 & 0 \\ 0 & 0 & 1 \end{bmatrix}\begin{bmatrix} v_{c_0}c_1 \\ -v_{c_0}s_1 \\ 0 \end{bmatrix} = \begin{bmatrix} v_{c_0}c_1c_2 - v_{c_0}s_1s_2 \\ -v_{c_0}c_1s_2 - v_{c_0}s_1c_2 \\ 0 \end{bmatrix} \tag{3-12} $$

$$ {}^{2}\dot{v}_2 = {}^{2}_{1}R\left(\dot{\omega}_1 \times {}^{1}p_2 + \omega_1 \times \left(\omega_1 \times {}^{1}p_2\right) + {}^{1}\dot{v}_1\right) \tag{3-13} $$

$$ v_{c_2} = \dot{\omega}_2 \times {}^{2}P_{c_2} + \omega_2 \times \left(\omega_2 \times {}^{2}P_{c_2}\right) + {}^{2}\dot{v}_2 \tag{3-14} $$

The ankle joint is defined as joint 3. Its velocity and acceleration model are expressed by.

$$\omega_3 = {}^3_2R\omega_2 + \dot{\theta}_3\hat{Z}_3 = \begin{bmatrix} c_3 & s_3 & 0 \\ -s_3 & c_3 & 0 \\ 0 & 0 & 1 \end{bmatrix}\begin{bmatrix} 0 \\ 0 \\ \dot{\theta}_1 + \dot{\theta}_2 \end{bmatrix} + \begin{bmatrix} 0 \\ 0 \\ \dot{\theta}_3 \end{bmatrix} = \begin{bmatrix} 0 \\ 0 \\ \dot{\theta}_1 + \dot{\theta}_2 + \dot{\theta}_3 \end{bmatrix} \tag{3-15}$$

$$\dot{\omega}_3 = {}^3_2R\dot{\omega}_2 + {}^3_2R\omega_2 \times \ddot{\theta}_3\hat{Z}_3 + \ddot{\theta}_3\hat{Z}_3 = \begin{bmatrix} 0 \\ 0 \\ \ddot{\theta}_1 + \ddot{\theta}_2 + \ddot{\theta}_3 \end{bmatrix} \tag{3-16}$$

$${}^3v_3 = {}^3_2R\left({}^2\omega_2 \times {}^2P_3 + {}^2v_2\right) \tag{3-17}$$

$${}^3\dot{v}_3 = {}^3_2R\left({}^2\dot{\omega}_2 \times {}^2P_3 + {}^2\omega_2 \times \left({}^2\omega_2 \times {}^2P_3\right) + {}^2\dot{v}_2\right) \tag{3-18}$$

$$\dot{v}_{c_3} = \dot{\omega}_3 \times {}^2P_3 + \omega_3 \times \left(\omega_3 \times {}^3P_{c_3}\right) + {}^3\dot{v}_3 \tag{3-19}$$

The hydrodynamic force under fixed coordinates is expressed below.

$${}^0f_w = C^*\rho A v_{c_3}\left|v_{c_3}\right| \tag{3-20}$$

where C^* are the drag and lift coefficient (C_D, C_L) of the webbed foot, ρ is the density of water, and v_{c_3} is the velocity of the mass centre of the foot.

The force on joint 3 is calculated as follows.

$${}^3f_3 = {}^3f_w + {}^3F_3 \tag{3-21}$$

where ${}^3F_3$ is the inertia force, which is expressed as ${}^3F_3 = m_{c_3}\dot{v}_{c_3}$.

The torque on joint 3 is:

$${}^3n_3 = {}^3P_{c_3} \times \left({}^3F_3 + {}^3f_w\right) \tag{3-22}$$

The forces and torque on the other joints are as follows.

$${}^2n_2 = {}^2_3R \cdot {}^3n_3 + {}^3p_3 \times {}^2_3R \cdot {}^3F_3 \tag{3-23}$$

$${}^2F_2 = {}^2_3R \cdot {}^3F_3 + m_2\dot{v}_2; \tag{3-24}$$

$${}^1n_1 = {}^1_2R \cdot {}^2n_2 + {}^2p_2 \times {}^1_2R \cdot {}^2F_2 \tag{3-25}$$

$${}^1F_1 = {}^1_2R \cdot {}^2F_2 + m_1\dot{v}_1 \tag{3-26}$$

$${}^0n_0 = {}^0_1R \cdot {}^1n_1 \tag{3-27}$$

$${}^0F_0 = {}^0_1R \cdot {}^1F_1 \tag{3-28}$$

where ${}^0F_0$ and ${}^0n_0$ are the force and torque on the hip joint.

3.2 Force modelling of the robot body

The robot body is subject to water fluid force during robot swimming. The force is determined by the flow field which is generated by the interaction between the swimming robot and the water and is difficult to model by theoretical calculation and experiments. Here we use the fluid simulation to model the fluid force on the robot body with the CFD software.

3.2.1 Grid generation of the body in the fluid simulation

Grid generation is shown in Fig. 5. The outflow field is automatically divided by tetrahedral grid and three prismatic layers are added at the interface of the body surface to improve the calculation accuracy. The simulation adopts steady-state mode with the flow inlet on the left and the pressure outlet on the right, and the flow velocity changes.

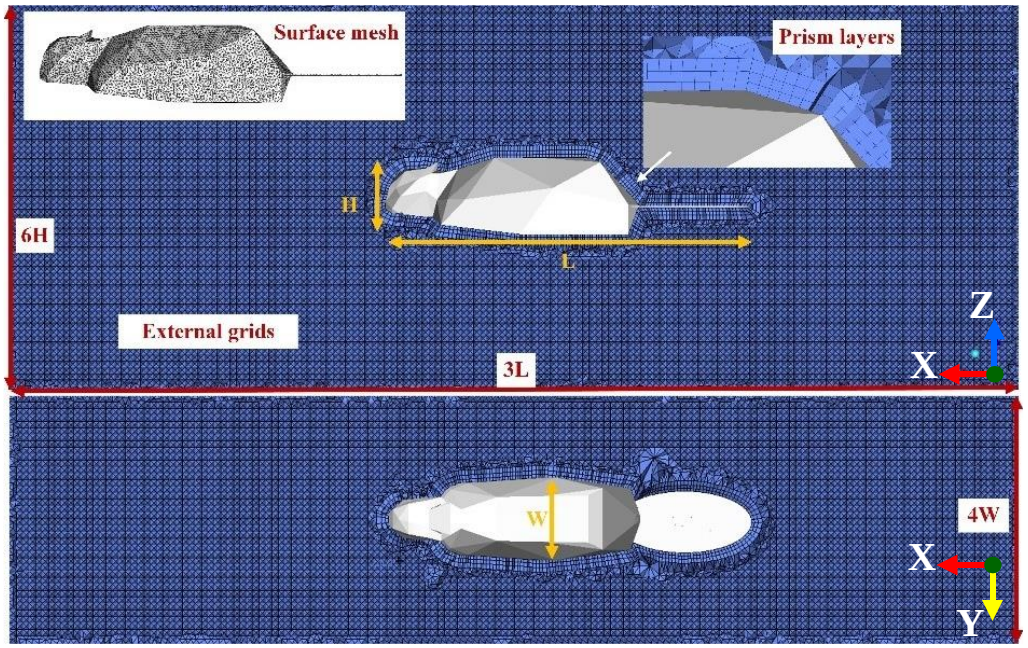

Fig. 5 Grid division of body in outflow field

3.2.2 Force model of the body with fluid simulation results

Fig. 6 shows the outer shell of the body in the flow velocity cloud diagram of the outflow field. As can be seen, the velocity of the flow field at the head and back of the shell is large and the flow is relatively static at the tail. The simulations were conducted with the flow velocity increasing from 0 m/s to 1 m/s. The fluid forces on the body of the robot are drawn in Fig. 7.

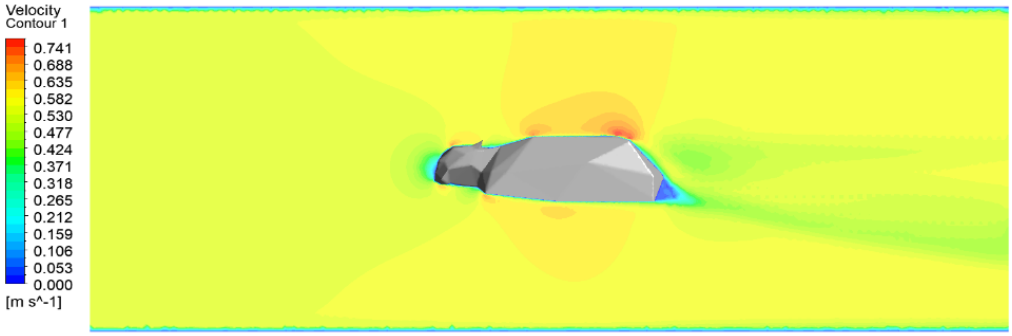

Fig.6 Flow velocity cloud diagram of the outflow field

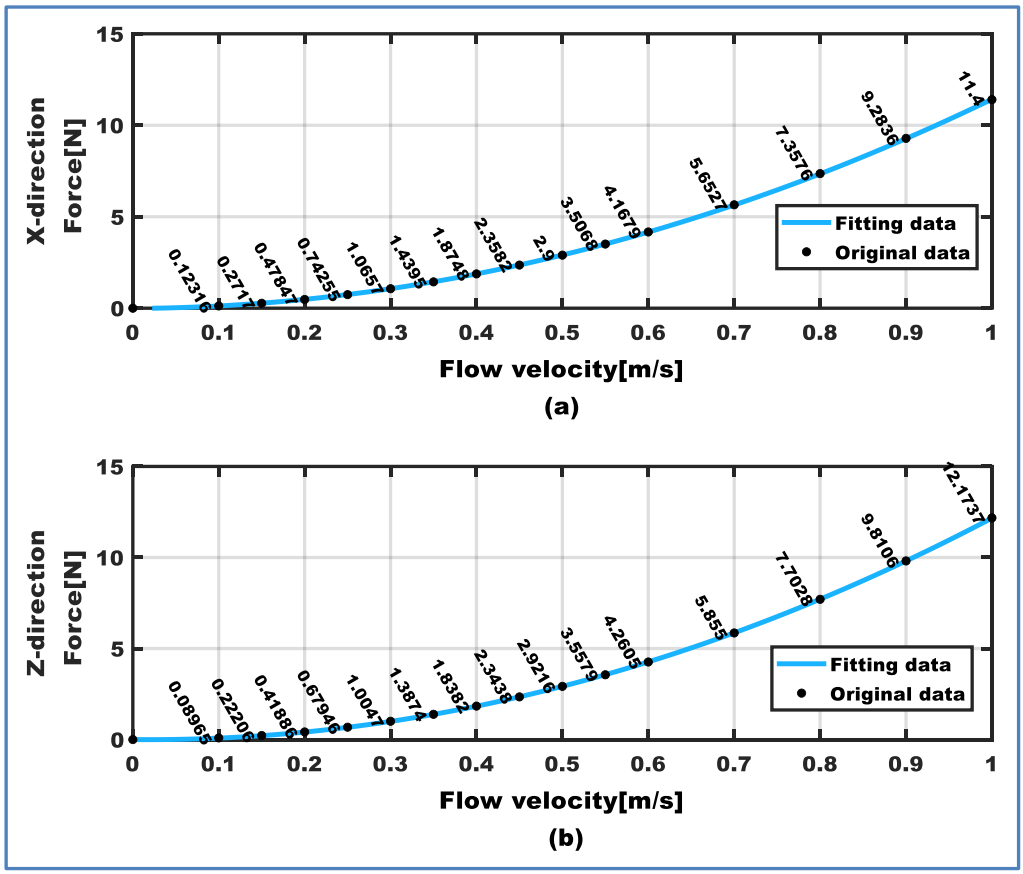

Fig. 7 Force on the body in the XZ direction in fluid simulation

The simulation results are fit by a second order polynomial, and the fluid force on the body of the robot can be obtained as follows.

$$F_{kx} = 11.2v^2 + 0.2v \tag{3-29}$$

$$F_{kz} = 12.6v^2 - 0.5v \tag{3-30}$$

where v is the velocity of the fluid.

3.3 Dynamic modelling of swimming posture of beaver-like robot

Newton Euler equations were used to model the dynamics of webbed foot, leg, tail, and whole of the robot. [39, 40]. Fig. 8 shows the coordinate system of the robot, namely the global coordinate system {W} and the body coordinate system {B}.

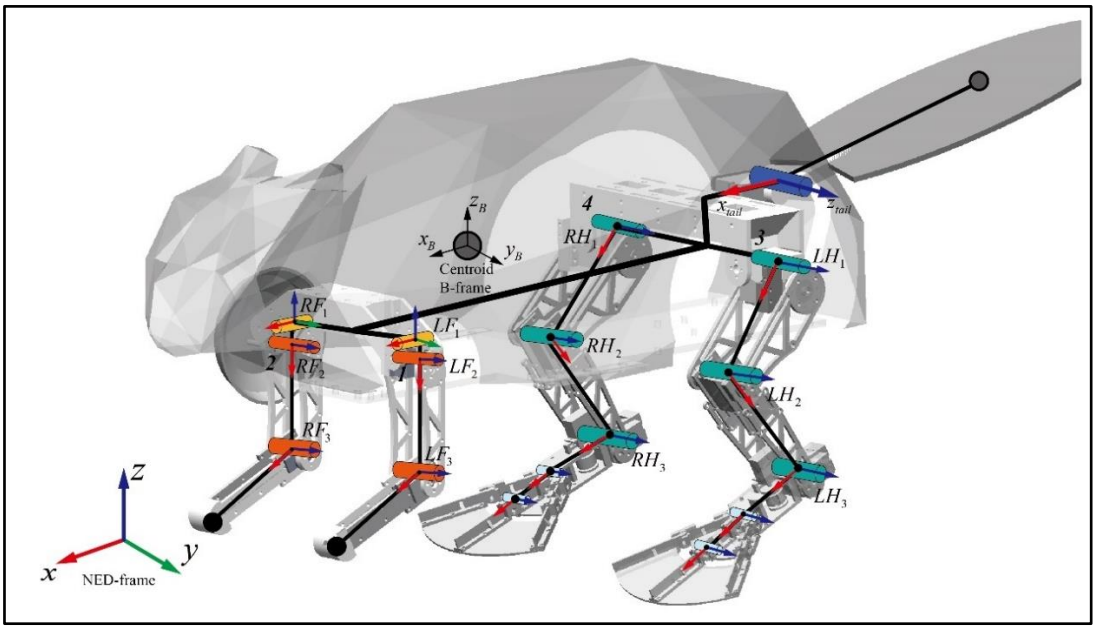

Fig. 8 Overall DH parameters of our beaver-like robot

Thus, the inertial matrix M_{RB} of the robot can be obtained by using

$$M_{RB}=\begin{bmatrix} 4.35 & 0 & 0 & 0 & 0 & 0 \\ 0 & 4.35 & 0 & 0 & 0 & 0 \\ 0 & 0 & 4.35 & 0 & 0 & 0 \\ 0 & 0 & 0 & 0.21 & 0 & 0.0015 \\ 0 & 0 & 0 & 0 & 0.28 & 0 \\ 0 & 0 & 0 & 0.0019 & 0 & 0.32 \end{bmatrix} \tag{3-31}$$

Considering the low swimming velocity of the robot, the inertia matrix can be simplified as:

$$M_{RB}=diag\{[4.35 \quad 4.35 \quad 4.35 \quad 0.21 \quad 0.28 \quad 0.32]\} \tag{3-32}$$

The coordinate point of leg 3 in the motion coordinate system $X_BY_BZ_B$ (body) is:

$$P_3=\begin{bmatrix} l_b \\ h_b \\ w_b \end{bmatrix} \tag{3-33}$$

Then the force/moment of the single hip joint on the centre of mass of the body is F_0 and $F_0\times P_3+n_0$. The coordinate point of the corresponding joint in leg 4 is:

$$P_4 = \begin{bmatrix} l_b \\ -h_b \\ w_b \end{bmatrix} \tag{3-34}$$

The force/moment at the centre of mass of hip joint 3 and 4 is τ_{hip}:

$$\tau_{hip} = \begin{pmatrix} F_{(4)0} + F_{(3)0} \\ \mathbf{0}^{1\times 3} \end{pmatrix} + \begin{pmatrix} \mathbf{0}^{1\times 3} \\ F_{(4)0} \times p_4 + F_{(3)0} \times p_3 + {}^0n_{(3)0} + {}^0n_{(4)0} \end{pmatrix} \tag{3-35}$$

where $F_{(4)0}$ and $F_{(3)0}$ are related to the posture of the leg joints and the velocity of the webbed foot at that moment.

According to the force model of the body, the comprehensive hydrodynamic force received by the underwater robot in swimming is:

$$\tau_{shell} = \begin{bmatrix} F_{kx} \\ F_{ky} \\ F_{kz} \end{bmatrix} = \begin{bmatrix} 11.2v^2 + 0.2v \\ 0 \\ 12.6v^2 - 0.5v \end{bmatrix} \tag{3-36}$$

Then, the resultant force/torque of the robot's body in swimming is:

$$\tau = \tau_{shell} + \tau_{hip} \tag{3-37}$$

Thus, the posture dynamic model of robot in swimming can be obtained below:

$$M_{RB}\dot{v}(t) = \tau \tag{3-38}$$

Further, the swimming posture of the robot can be obtained as follows.

$$\dot{v}(t) = M_{RB}^{-1}\tau \tag{3-39}$$

$$v(t) = \int (M_{RB}^{-1}\tau)\, dt \tag{3-40}$$

$$\eta(t) = \int\int (M_{RB}^{-1}\tau)\, dt \tag{3-41}$$

4. Simulation of swimming posture dynamics model of our beaver-like robot

Fig. 9 shows a beaver-like robot prototype model established in ADAMS. The paddling force of webbed foot and fluid force on body were obtained through Fluent simulation were added to the ADAMS model. The two motion modes of the robot, namely alternating and synchronous swimming, were simulated respectively to obtain the torques of the hip, knee, and ankle joint and the posture (pitch, yaw, and roll) of the robot in the process of moving forward. Then, the results are compared with those obtained by theoretical modelling in MATLAB to verify the correctness of the swimming posture dynamics modelling of the

robot.

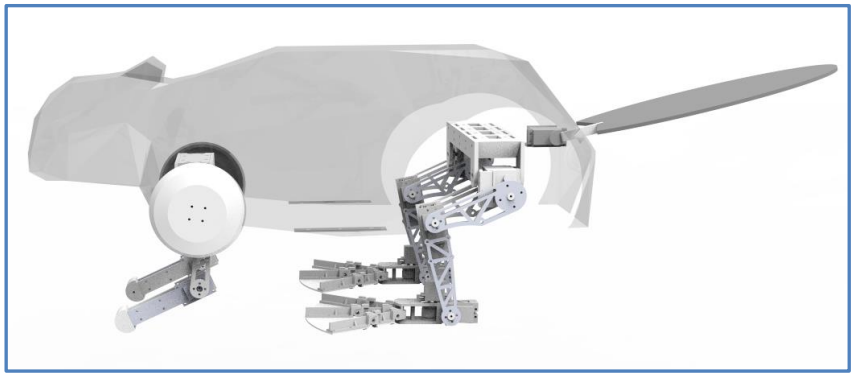

(a)

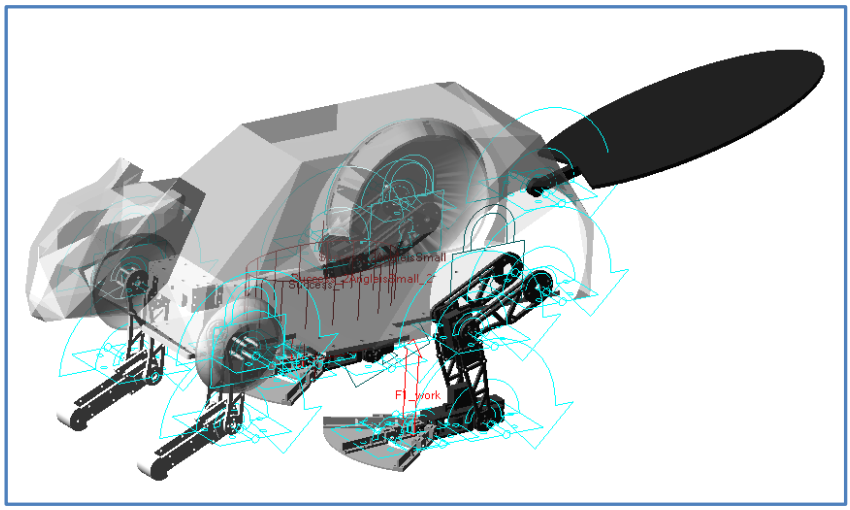

(b)

Fig. 9 ADAMS simulation model of our beaver-like robot

Fig. 10 shows the posture changes with the alternate swimming mode of the beaver-like robot. In the first 10 seconds, both the robot posture errors between theoretical and simulation results fluctuate greatly, and the errors reach the peak value 18° in yaw direction. The main reasons for this phenomenon are as follows. When the robot initially moves from a static state, the fluid resistance has a rapid nonlinear change in a short time, which cannot be accurately computed in the theoretical model. After several cycles of motion, the hydrodynamic force generated by the webbed foot paddling and the additional mass force and resistance reach a relatively stability state. The attitude error stably mains in a range of 0-5°. The trend of posture in roll and pitch direction is like the posture in the yaw direction, and their amplitude changes are small as the hydrodynamic forces generated by the two with alternate paddling webbed feet partly cancel each other out.

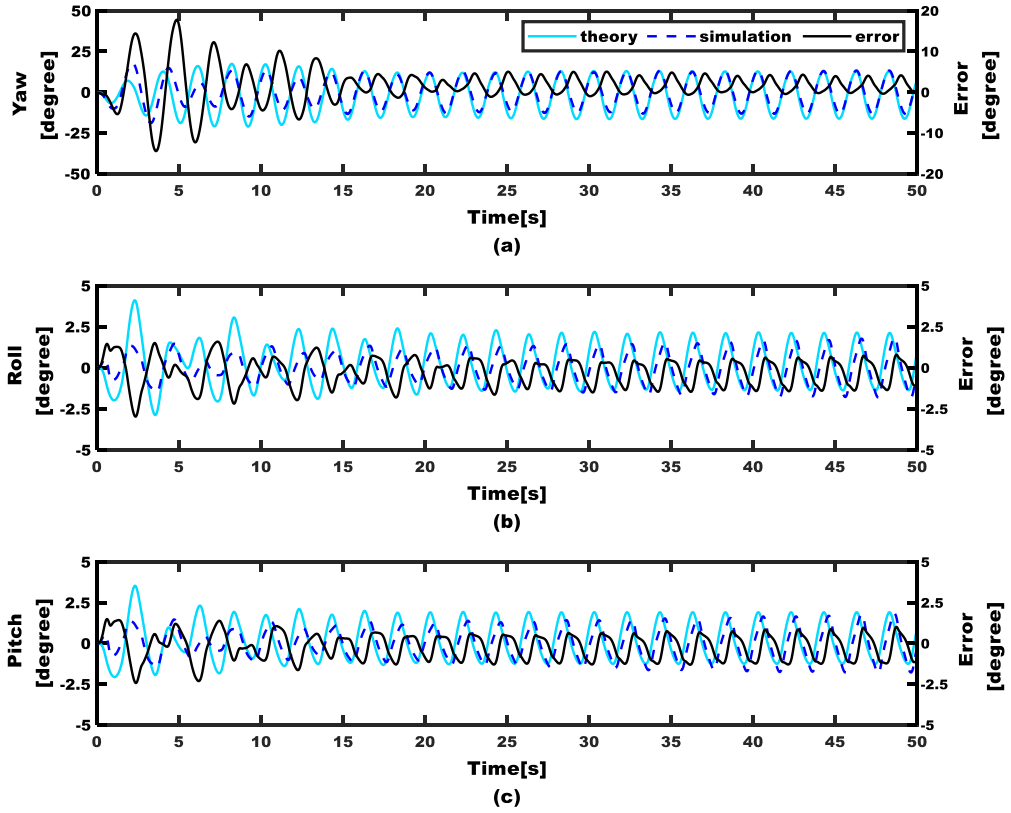

Fig. 10 Posture of the beaver-like underwater robot in alternate swimming

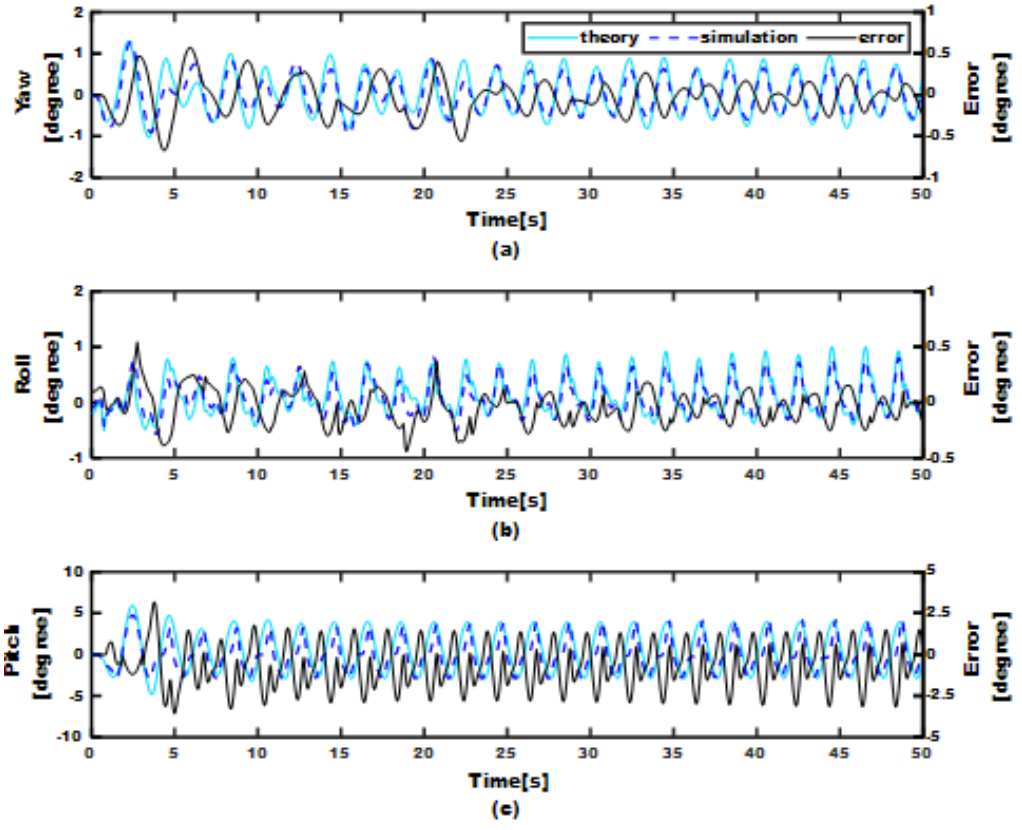

Fig. 11 Attitude change curve of beaver-like underwater robot in synchronous swimming

Fig. 11(a) and (b) show the posture amplitudes in yaw and roll direction change small. because the hydrodynamic forces generated by the webbed feet with synchronous paddling partly cancel each other out in synchronous motion of the robot. In the pitch direction, a relatively moment is generated due to the synchronous paddling of the webbed feet. Thus, a large change in pitch amplitude reach 7°, but it is smaller than that of yaw amplitude. The reason is that the rotational inertia in pitch direction is larger than that in yaw direction.

5. Swimming experiments of the beaver-like underwater robot

Fig. 12 and Fig. 13 show the movement process of the beaver-like underwater robot with alternate and synchronous swimming modes respectively. In alternate swimming, two hind limbs of the robot propel the body forward by alternate paddling. In one movement cycle, two webbed feet provide propulsion force alternately so that the body can continue moves. The movement process is relatively stable, and the pitch angle does not change largely, maintaining in the range of 1°-6°. In synchronous swimming, two hind limbs of the robot move forward synchronously. In one movement cycle, the two webbed feet provide propulsion force and withstand the resistance of water flow at the same time. As the propulsion force is not continuous, the movement process is not smooth, and the pitch angle changes greatly, reaching 13°. Through the alternate and synchronous swimming experiments, the characteristics of posture change in different swimming modes of the robot were verified, and the necessity of the dynamic analysis of swimming posture and the correctness of the model are further demonstrated.

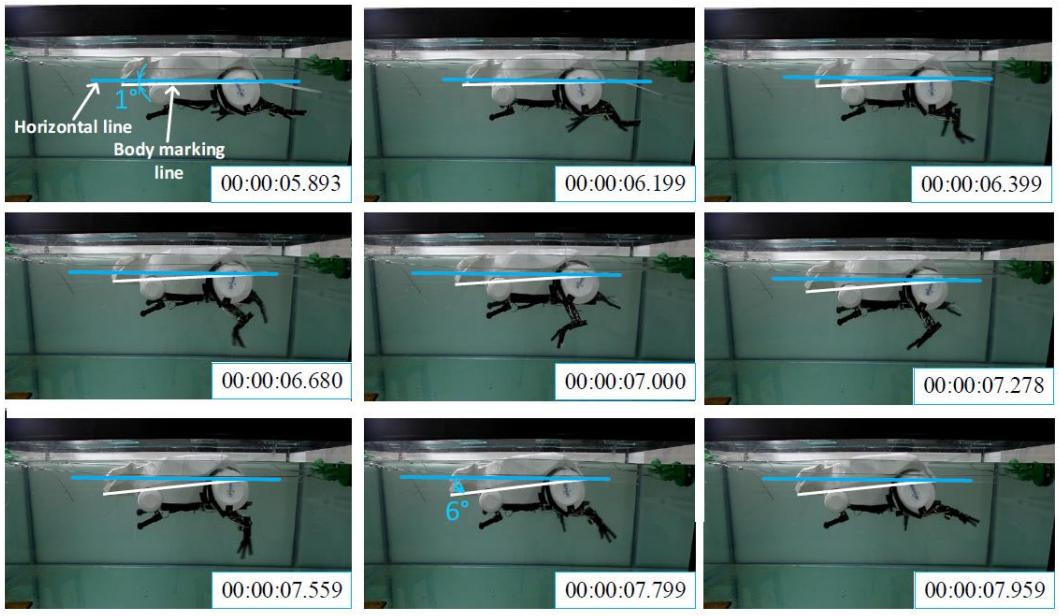

Fig. 12 Alternate swimming experiment of our beaver-like robot

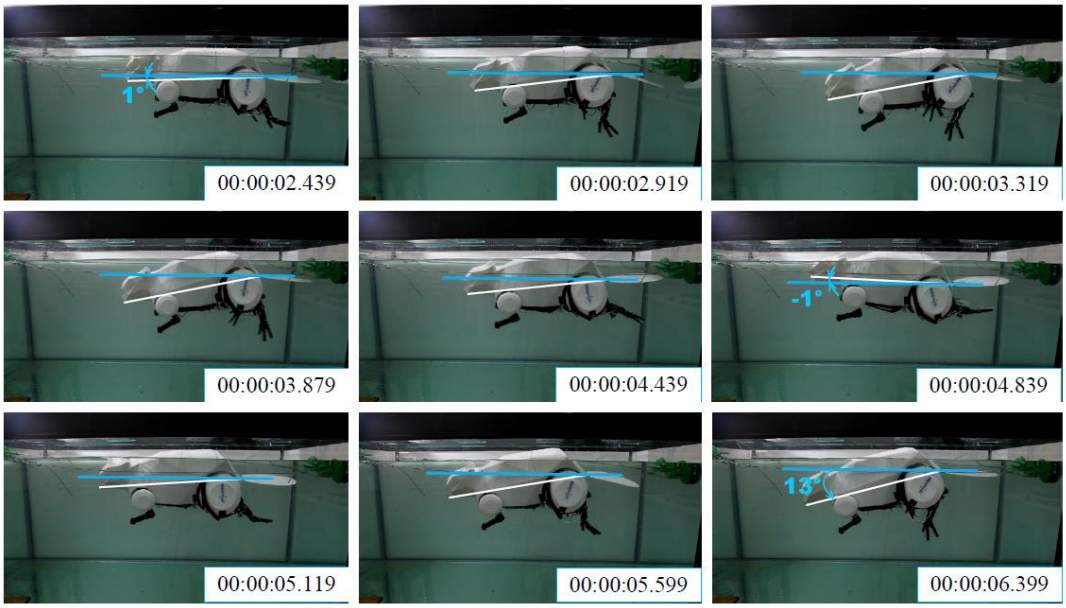

Fig. 13 Synchronous swimming experiments of our beaver-like robot

6. Conclusions

This paper presents the development of a beaver-like robot. Its rigid body dynamics and hydrodynamics were integrated to establish the leg dynamics model of the robot. Its body hydrodynamics was then analysed based on Fluent simulation. The force of leg dynamics and body hydrodynamics on the robot body was further integrated. Finally, its swimming posture dynamic model was established. ADAMS simulation and prototype experiments were conducted to verify the rationality and correctness of the swimming posture dynamics model in different swimming modes of the robot.

The main conclusions are summarized below.

1) By comparing the simulation and model calculation results of the swimming postures of the beaver-like robot in the alternate and synchronous swimming modes, it is found that they are basically consistent when the swimming is stable in simulation. The maximum errors of yaw are 4.46°and 0.54° respectively. The maximum errors of roll are 1.59° and 0.54°, respectively. The maximum error of pitch is 1.50° and 3.15° respectively. It is proved that the swimming posture dynamics modelling method of the robot is correct and effective.
2) In the alternate swimming, the yaw angle of the robot changes greatly, and the pitch angle varies largely in the synchronous swimming. The characteristics of the robot's posture change under these two swimming modes are verified by the robot's swimming posture dynamics.

3) The alternate and synchronous swimming of our beaver-like robot have different effects on its posture. It is an important way to keep a stable posture and change the motion mode reasonably according to the water environment and its current posture.

In the future, a posture sensor will be installed in our beaver-like robot prototype, and the adaptive posture control under water flow disturbance will be studied based on the robot posture information.

Acknowledgements

This work was financially supported by National Natural Science Foundation of China (No. 51875528), Zhejiang Provincial Natural Science Foundation of China (No. LY20E050018), Natural Science Foundation of Zhejiang Province (No. LTY21F030001), and Science Foundation of Zhejiang Sci-Tech University (ZSTU) (No. 17022183-Y).

References

[1] Johansson L C, Norberg R A. Delta-wing function of webbed feet gives hydrodynamic lift for swimming propulsion in birds[J]. Nature, 2003,424(6944):65-68.

[2] Nir S, Ruchaevski I, Shraga S, et al. A jellyfish-like robot for mimicking jet propulsion: IEEE convention of electrical and electronics engineers in Israel, 2012[C].2012.

[3] Yu J, Yuan J, Wu Z, et al. Data-Driven Dynamic Modelling for a Swimming Robotic Fish[J]. IEEE Transactions on Industrial Electronics, 2016,63(9):5632-5640.

[4] Roper D T, Sharma S, Sutton R, et al. A review of developments towards biologically inspired propulsion systems for autonomous underwater vehicles[J]. Proceedings of the Institution of Mechanical Engineers, 2011,225(2).

[5] Richards C T, Clemente C J. Built for rowing: frog muscle is tuned to limb morphology to power swimming[J]. Journal of the Royal Society Interface, 2013,10(84):20130236.

[6] Stamhuis E and Nauwelaerts S. Propulsive force calculations in swimming frogs II. Application of a vortex ring model to DPIV data[J]. Journal of Experimental Biology, 2005,208(8):1445-1451.

[7] Jizhuang F, Wei Z, Bowen Y, et al. Propulsive efficiency of frog swimming with different feet and swimming patterns[J]. Biology Open, 2017,6(4):503-510.

[8] Allers D and Culik B M. Energy Requirements of Beavers (Castor Canadensis) Swimming Underwater[J]. Journal of Physiological and Biochemical Zoology, 1997,70(4):456-463.

[9] Fish F E. Mechanics, power output and efficiency of the swimming muskrat (Ondatra zibethicus)[J]. Journal of Experimental Biology, 1984,110:183.

[10] Havahart, https://www.pinterest.com/pin/23362491805226228/,2021,11